 SDHM, vol.5, no.4, pp.337-349, 2009

The Residual Stress State Due to Machining of Turbine Components: Experimental Investigation

M. Lavella[1] **and T. Berruti**[1]

Abstract: Results of residual stress measurements on Inconel 718 turbine components after machining are here presented. The work is focused on the experimental detection of the residual stress state produced after turning (orthogonal cutting and standard) and milling. The aim of the experimental activity was to supply an experimental data base of proved reliability for milling and turning model validation. This activity was performed inside the EU STREP project VERDI. The residual stresses were detected by means of X-ray diffraction technique. The experimental plan of measurements was performed on components worked with different working parameters (cutting velocity and feed rate) and by means of new and worn tool. The trends of residual stress versus depth are presented.

Keywords: turning, milling, residual stress, X-ray diffraction.

1 Introduction

The present work is focused on the experimental detection of the residual stress state produced after turning and milling in turbine components made of Inconel 718. The work is part of the experimental activity for the EU STREP project named VERDI (Virtual Engineering for Robust Manufacturing with Design Integration) which aims at producing an efficient numerical model for prediction of the stress state due to the machining and to other manufacturing processes. VERDI includes also life prediction based on the as-manufactured state of the component. An example of a correlation between residual stresses and machining can be found in Capello, Davoli, Filippini, and Foletti, (2004). The experimental results here presented are part of an experimental data base produced for numerical models validation. The obtained results give some indications about the distribution of residual stresses with particular care to the presence of tensile stress after working using the working parameters of the industrial best practice. The studies on residual stress state induced in Inconel 718 by machining are not so numerous as for the steel and

[1] Dipartimento di Meccanica, Politecnico di Torino, Torino, Italy

often lead to apparently contradicting results. Sadat and Reddy (1992, 1993) analyze the case of turned orthogonal cut samples with the influence of lubrication, they find that surface residual stress values are tensile and increase with an increase in cutting speed (12 ÷ 97 m/min), in dry cutting conditions surface stresses are lower and not so influenced by the cutting speed value. Arunachalam, Mannan and Spowage, (2004) investigated the residual stress state (detected by means of X-ray diffraction) due to high speed facing operation. They found that with the increase in the cutting speed (150-375 m/min) the residual stress values changed from compressive to tensile values. Moreover they found that the insert geometry and the presence of coolant can affect the residual stress sign. Sharman, Hughes and Ridgway (2006) analyze the residual stress (detected by means of hole drilling technique) generated in Inconel 718 when turning, they show that the tool wear has the largest influence on residual stress distribution and value. In the present work the usual tool wear proves to be not so relevant for 'heavy' machining processes and to be more relevant for a finishing working. Pawade, Joshi, Brahamnkar and (2008) study the case of high speed turning, they measure residual stress by means of X-ray diffraction; as the cutting speed increases (125-300 m/min) the tensile residual stresses increase, but for higher values of cutting speed (300- 475 m/min) the residual stresses change sign from tensile to compressive.

From the above short overview it can be noticed that Inconel machining does not show just one trend of residual stress versus working parameters, i.e. residual stresses do not depend on the single factor but on a combination of factors. A so high sensitivity of results to factors requires an accurate estimate of experimental errors and a careful calibration. This was the guiding principle of this paper when determining the effect of process parameters on residual stresses. Due attention was given to the assessment of the uncertainty of experimental results.

2 Experimental equipment and samples

Residual stress measurement. The residual stress state was detected by means of an X Ray Diffractometer Siemens D5005, whose main technical features and measurement parameters are: fixed sample holder, rotating tube and detector, goniometer OMEGA θ - θ, Cr anode radiation, Bragg angle (2θ) 133.53, circular spot area diameter ϕ = 4 mm, dual Pearson VII peak interpolation.

Electrolytic material removal. In order to measure the residual stress state at different depths material layers were removed by means of electrolytic technique. After the removal the surface profile was detected by means of the test profile Profiltest R70 (estimated accuracy 1 μm).

Samples. The material is Inconel 718 heat treated by solution and aging according

to MSRR 7090 specification. The samples are obtained with the standard working parameters from the aerospace industrial best practice and they are cooled by coolant emulsified in water (5.5%) at 7 bar. The working parameters are listed in Table 1. The turned samples come from a raw low pressure turbine shaft. A first batch of turned samples was obtained by means of an unusual turning condition: hollow cylinders are worked (1 pass) on their plane surface (as shown in Figure 1 a)). The idea was to reproduce the ideal case of "orthogonal cutting condition". In this case the ratio chip width (6 mm) on chip thikness (0.15 mm) is equal to 40 (which is intentionally high). The second batch of turned samples (Figure 1 b)) are hollow cylinders machined, as the standard practice, on the external diameter. On each sample 8 consecutive passes were performed. The milled samples (Figure 1c)) were extracted from a mock-up of a real low pressure turbine disk. Milling is used to create rounded 'scallops' on the disk, a design feature commonly used for stress redistribution and weight saving on flanges that can be found on turbine rotating parts and exhaust frames. On each sample 3 consecutive passes were performed.

Table 1: Samples working parameters.

	Depth of cut	Cutting velocity	Feed rate
TURNED samples (orthogonal cutting)	0.15 mm	35 m/min 50 m/min	0.15 mm/rev 0.2 mm/rev
TURNED samples (standard cutting)	0.30 mm	50 m/min	0.30 mm/rev
MILLED samples	0.30 mm	35 m/min	0.22 m/min

The milling working here examined is the last working of the 'scallops', it can be considered as a 'finishing' working. The samples are worked by means of new and worn tools. In the case of turned samples the "worn" tool showed from a stereomicroscope picture a flank wear with an average width of approximately 150 μm. In the case of milled samples the "worn" tool showed an average width of approximately 50 μm (that is less wear than the case of turning).

3 The measurement uncertainty

The uncertainty of residual stress was estimated according to the analysis of the three different sources of error listed below.

The accuracy error, obtained as the difference of the measurement result and the "true" value of stress, this error was obtained by means of measurements on a stress free reference sample and on a sample with known stress value.

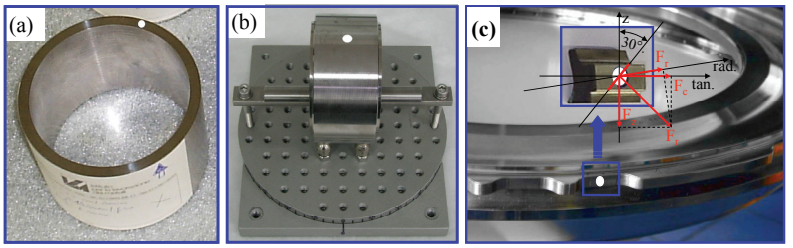

Figure 1: Inconel 718 samples a) TURNED sample (ORTHOGONAL CUTTING). b) TURNED sample (STANDARD CUTTING). c) MILLED sample.

The repeatability error obtained after removing and positioning the sample on the sample holder.

The error due to the propagation of the counting statistics error of the diffraction peaks in the data fitting procedure.

3.1 Accuracy error.

According with Standards SAE (1971), AFNOR (1999) and ASTM (2002) the measurement accuracy was checked by means of a stress free reference sample and by means of stressed samples (loaded by a device purposely designed and constructed).

The stress free reference sample is a layer of pure reduced iron powder (particle size 10 μm) as shown in Figure 2 a). The measurements were performed in three different φ directions: -60°,0°,+60°. Each set of measurements (in the three φ directions) was repeated three times after repositioning of the sample on the sample holder. The measurement was supposed to give a null stress value and this was confirmed by the detected stress values inside $\pm$ 2 MPa.

The sample with known stress value is a beam with a constant bending moment as shown in Figure 2 b). The applied stress is detected both by strain gages and by diffraction. The strain gages (SG) measurement is performed on the lower beam surface, while the diffractometer measurement is performed on the upper beam surface where the absolute value of the stress can be assumed to be the same. The sample loading device shown in Figure 2 b) has the following features:

- U-shaped portal loaded by means of a loading pin with spherical tip on a conical surface, the pin is driven by means of an index crank.

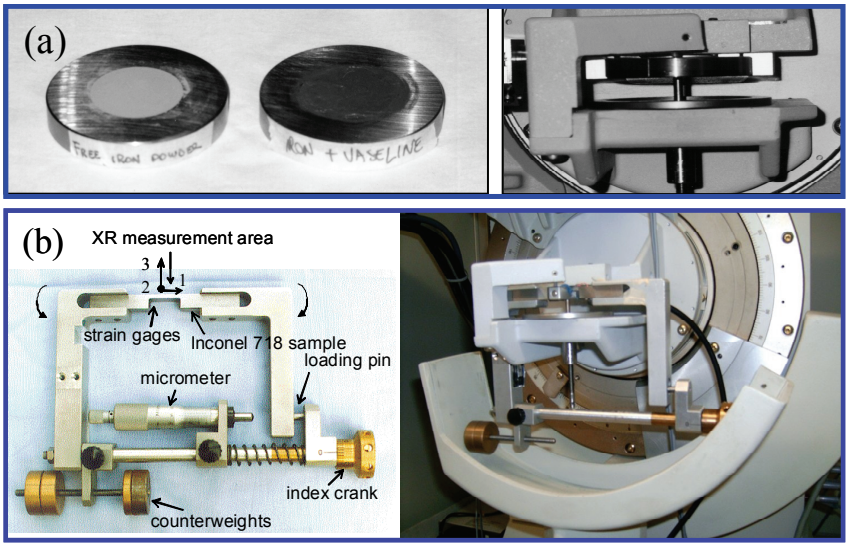

Figure 2: a) Stress free samples. b) Bending loading device.

- strain gages rosette (M-M, CEA-06-062UT-120 with two perpendicular gages, one gage along sample axis, one gage perpendicular to the sample axis (half bridge connection K = 1.87±1.5%, 120 Ω), the rosette is glued on the sample below the measurement area and give the stress value along the sample axis direction

- portal supported by a pin carried by the sample holder, the irradiated area of the sample (measurement area) is kept on the plane (focal reference plane) defined by the three diffractometer reference pins, the counterweights can be adjusted in order to keep the sample measurement surface parallel to the focal reference plane.

The X-ray stress in the measurement area is calculated by subtracting from the X-ray stress detected on the loaded sample the X-ray stress detected on the unloaded sample.

The average difference between strain gage stress value (assumed as reference) and the X-ray stress value is assumed as the accuracy error of the stress measurement. This error is computed first on a steel sample considered as the optimal case with Cr anode radiation and then on an Inconel sample (same alloy of the Inconel turned

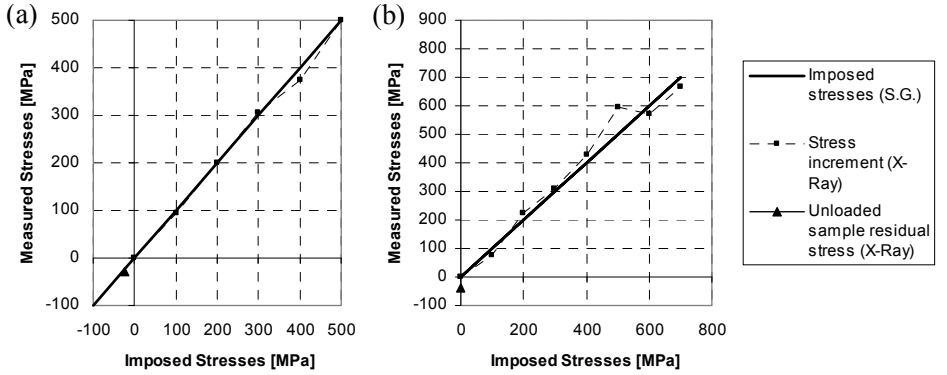

Figure 3: Comparison of SG and diffractometer measurements: (a) steel sample, (b) Inconel 718 sample.

samples). The measurements are repeated for 3 cycles of loading and unloading. Figure 3a) shows the comparison between strain gage stresses and X-ray stresses in the case of a steel sample, the average measurement difference being 7 MPa. Figure 3b) shows the same comparison in the case of a Inconel 718 sample, the average measurement difference, that is the estimated accuracy error, being 35 MPa. This highest error for Inconel compared to steel is due to higher uncertainty in the residual stress determination from diffraction peak shift due to lower Bragg angle (133° for Inconel against 156 for steel) and lower maximum ψ angle (40° for Inconel against 50° for steel).

3.2 Repeatability error

It was estimated by means of measurement repetition on the same point after removal and repositioning of the sample on the sample holder. The chosen sample was a turned sample with a mean stress value on the surface of 850MPa in tangential direction and 1050 MPa in longitudinal direction. The repeatability error on the sample surface proved to be higher in longitudinal than in tangential direction: the repeatability error was 80 MPa in longitudinal direction and about 20 MPa in tangential direction. The higher repeatability error in the longitudinal direction is related to the higher scatter of the diffracted peaks in this direction. An hypothesis is that the higher scatter of the diffracted peaks detected in longitudinal direction is caused by the presence of working debris at the tip of the working marks (that have tangential direction). The basic idea is that these debris could influence the diffraction in the direction normal to the working marks (i.e. the longitudinal direction) causing scatter in the diffracted peaks. This hypothesis was confirmed

by the measurements performed after electrolytic removal when the scatter of the diffracted measured peaks clearly decreased: a removal of $2 \div 3$ μm was enough to observe diffracted peaks more clean than at the machined surface. This experimental evidence might support the idea of considering the working debris rather than the surface roughness as the cause of the peaks scatter since after a removal of $2 \div 3$ μm the surface roughness does not change.

As a consequence the repeatability error decreases when the measurements are performed after electrolytic removal. After electrolytic removal at different depths the repeatability error stabilized to a value of 30 MPa without a meaningful difference between the two measurement directions.

3.3 Error for counting statistics

This error is calculated as a consequence of the propagation of error in the data fitting procedures. Each point of a diffraction peak is a number of counts N with an error due to the counter statistics that is usually assumed as $\delta I = (N/\tau^2)^{1/2}$ (Noyan and Cohen (1987)) where τ (20 s) is the acquisition time. This error propagates through the peak fitting (by Pearson VII) and through the ellipse interpolation of the peak maximum positions. This error is related to the diffracted peaks scatter and it increases with the increment of the peaks scatter. For the sample under test this error results to be in longitudinal direction, (direction with higher scatter), 120 MPa (on a mean value of 1050 MPa) and 70MPa in tangential direction (on a mean value of 850 MPa).

3.4 Estimate of the stress measurement uncertainty

The error on the final residual stress value due the propagation of the counting statistic error in the data fitting procedures resulted to be higher than the other two errors (accuracy and repeatability). It was than concluded that the uncertainty of the residual stress value due to accuracy and repeatability could be considered included in the uncertainty due to the counting statistics of the diffraction peaks (that is due to the scatter of the diffracted peaks). It was then chosen to associate to each residual stress measurement value an error that is the error due to counting statistic (as explained in section 3.3). Since the error is due to the peak scatter it must be computed each time that a residual stress value is determined from the diffracted peaks. As an order of magnitude it can be said that this error results to be in most cases about 10% of the stress value.

3.5 Estimate of the depth measurement uncertainty

The electrolytic technique removes material layers forming a groove slightly wider than the measurement area. The points on the groove bottom have different depths

respect to the original surface (before removal). A method has been adopted in order to determine a suitable average value of depth across the measurement area and to estimate the depth uncertainty. The method requires to measure three profiles after each removal by means of a profilometer. The three profiles (p_0, p_1 and p_2) are sketched in Figure 4 a) approximated by linear splines.

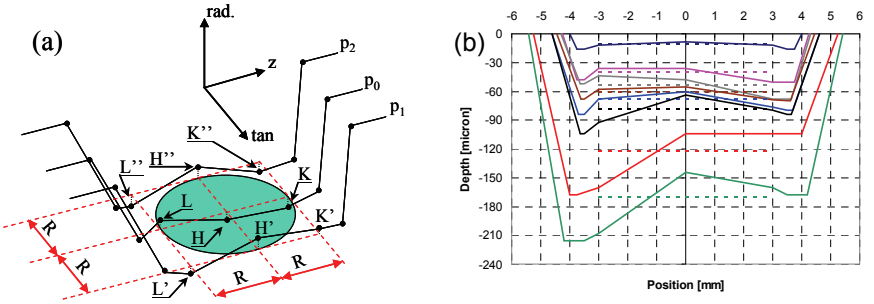

Figure 4: a) Sketch for mean depth calculation. b) Average electrolytic removal profiles.

The average profile of p_0, p_1 and p_2 is the average profile after each removal. The average profiles after different material removals are diagrammed in Figure 4 b). The depth value to be linked to the measurement stress values, is calculated as the mean value of the profiles in the nine points across the measurement area shown in Figure 4 a) (that is the average of the depth values of the nine points L, L', L", H, H', H", K, K', K"). The depth uncertainty is estimated as the standard deviation of the nine values. These average depth values after different removals are diagrammed as dotted lines in Figure 4 b).

4 Results and discussion

Measurement of residual stress were performed at different depths after electrolytical removal in order to produce the diagrams residual stress vs. depth for turned and milled samples in case of new and worn tool working.

Turned samples (orthogonal cutting). As shown in Figure 5 a) the stress profiles in both directions are tensile at the surface, with increasing depth beneath the workpiece surface the stress rapidly drops to a compressive level. Approximately 25 μm of material below the surface shows tensile stress. The highest value of compressive residual stress can be found between 25 and 50 μm. As shown in Figure 5b) the stress on the surface is still tensile also by varying working parameters (feed

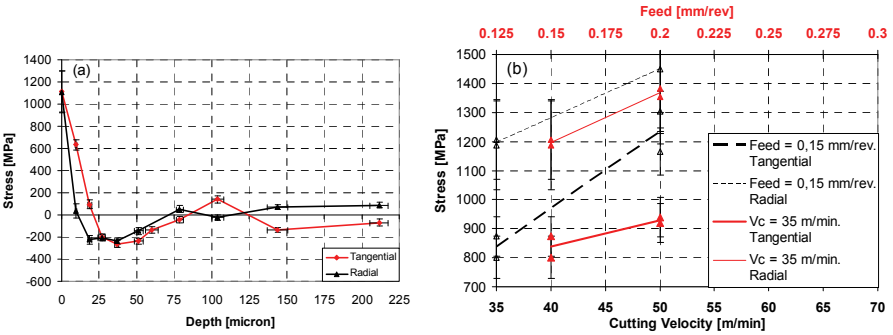

Figure 5: Stress measurements on Inconel 718 TURNED samples (ORTHOGONAL CUTTING - a) stress profile. b) surface residual stress vs. cutting parameters.

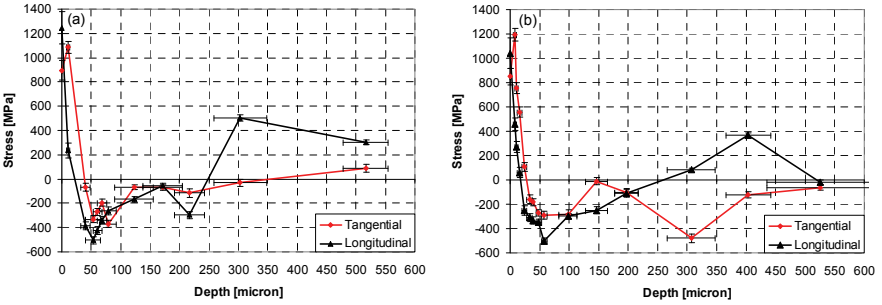

Figure 6: Stress profile on Inconel 718 TURNED samples (STANDARD CUTTING). a) NEW tool. b) WORN tool.

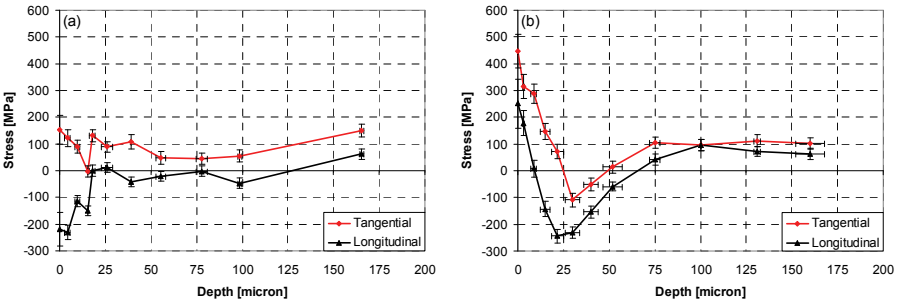

Figure 7: Stress profile on Inconel 718 MILLED samples. a) NEW tool, b) WORN tool.

rate and cutting velocity). By increasing the working parameters the surface stress value seems to increase.

Turned samples (standard working). From comparison of stress profiles caused by new and worn tool, respectively Figs. 6 a) and 6 b), it can be noted that they appear very much alike for both tangential and longitudinal directions.

In the typical depth range interested by the turning (from 0 to 150÷200 μm), there is not an evident difference among the two profiles. The shape of the profile is similar to the stress profile obtained on the first batch of turned samples (orthogonal cutting), but in this case about 50 μm of material below the surface shows tensile stress. With increasing depth beneath the workpiece surface the stress rapidly drops to a compressive level whose highest value is between 50 and 100 μm. The stresses in longitudinal direction return to tensile values after 200 μm while the stresses in tangential direction remain at compressive or small tension values. It must be said that considerations on the stress profiles for depth values higher than 200 μm are not so important since at this depth the stresses are not caused by the turning process but by the previous working processes (like the forging).

Milled samples. When cutting with new tool (Figure 7 a)) the stress profile shows positive stress in tangential direction (feed direction) and negative in longitudinal (disk axis) direction.

Tangential stress is kept almost constant at a low value of tensile stress (around 100 MPa). Axial stress is compressive at the surface and rapidly (at about 10-25 μm) reaches values around zero. When cutting with worn tool the stress profiles become more similar to the turning cases. In both directions the stress is tensile at the surface, with increasing depth beneath the workpiece surface the stress rapidly drops to a compressive level (at about 25 μm) before slowly returning to small tension values (after 50 μm). The stress profiles in tangential and longitudinal direction are in both cases (new and worn tool) almost always separated by a constant shift. This constant shift should be probably due to the different cutting forces (F_t and F_z) in tangential and longitudinal directions which have a constant ratio function of the cutting edge orientation as shown in the force sketch of Figure 7c). Similar profiles to those obtained by means of new tool in milling, have been found on milled carbon steel by Buzid Sai, Ben Salah, and Lebrun (2001). They found positive stress in feed direction whose values are influenced by the cutting speed value (by decreasing the cutting speed the profile was getting flat) and negative stress perpendicular to feed direction with a peak on the surface. The trends of the profiles obtained on turned samples and on the milled sample worked by worn tool confirm other trends found in literature by Sadat and Reddy (1992); Dahlman, Gunnberg and Jacobson (2004); M'Saoubi, Outeiro, Changeux, Lebrun, and Morao Dias (1999); Aspinwall, Dewes, Ng, Sage, and Soo (2007). These trends can be justify by an analysis

of the mechanisms leading to the generation of residual stresses. The generation of residual stress is determined by thermo-mechanical phenomena close to the tool tip as explained and modelled from Valiorgue, Rech, Hamdi, Gilles and Bergheau (2007). According to this model the thermal load is due to the heat flux coming from the primary shear zone and to rubbing effect. In this case due probably also to the poor thermal conductivity of Inconel 718 the sign of the surface residual stresses (tensile) shows that on the surface the thermal effect prevails against the mechanical effect. The developed high temperature causes stress similar to those due to thermal treatments that is surface tensile stress and compressive stress state beneath the thermally affected surface layer.

5 Conclusions

Particular attention to the measurement results errors was here paid since the experimental data will be used to verify and calibrate numerical models. The stress uncertainty due to different sources of errors was determined since the model specialists need to know both the experimental stress values and their uncertainty. From the observation of the experimental results the main guidelines that can be drown are:

turning (both in the case of orthogonal and standard cutting) and milling of Inconel 718, when performed according to the standard industrial best practice, induce a tensile residual stress with a crossover to a compressive regime between 10 and 50 μm beneath the surface, the trend seems to be an increment of the surface tensile value by increasing the cutting velocity and feed rate; it could than be suggested to perform a post process mechanical or surface treatment to remove these tensile stresses;

the usual tool wear seems to be relevant only in the case of milling, that in this case is a 'light' machining process (finishing working); in the case of an 'heavy' machining process, like the turning here considered, the examined level of wear does not influence the residual stress state.

Acknowledgement: The authors are grateful to EU for financing this work in the FP6 STREP VERDI project. Moreover the authors express their thanks to Mr. M. Cherubini of Avio Propulsione Aerospazio S.p.a. - Aeroengines division - Industrial Technologies Dept. for his collaborative support in the technological planning and manufacturing of the turned and milled samples.

References

AFNOR Normalisation francaise XP A 09-285 (1999): Méthods d'essais pour l'analyse des contraintes résiduelles par diffraction des rayons X.

Arunachalam, R.M.; Mannan, M.A.; Spowage, A.C. (2004): Residual stress and surface roughness when facing age hardened Inconel 718 with CBN and ceramic cutting tools. *Machine Tools & Manufacture*, vol. 44, pp. 879-887.

Aspinwall, D.K.; Dewes, R.C.; Ng, E.-G.; Sage, C.; and Soo, S.L. (2007): The influence of cutter orientation and workpiece angle on machinability when high-speed milling Inconel 718 under finishing conditions. *Machine Tools & Manufacture*, vol. 47, p. 1839-1846.

ASTM Standard E915-96 (2002): Test Method for Verifying the Allignment of X-Ray Diffraction Instrumentation for Residual Stress Measuremen, ASTM International, West Conshohocken, PA, DOI: 10.1520/E0915-96R02.

Buzid Sai, W.; Ben Salah, N.; Lebrun, J.L. (2001): Influence of machining by finishing milling on surface characteristics. *Machine Tools & Manufacture*, vol. 41, pp. 443-450.

Capello, E.; Davoli, P.; Filippini, M.; Foletti, S. (2004): Relaxation of residual stresses induced by turning and shot peening on steels. *Journal of Strain Analysis for Engineering Design*, vol. 39, pp. 285-290.

Dahlman, P.; Gunnberg, F.; Jacobson, M. (2004): The influence of rake angle, cutting feed and cutting depth on residual stresses in hard turning. *Journal of Materials Processing Technology*, vol. 147, pp. 181-184.

M'Saoubi, R.; Outeiro, J.C., Changeux, B.; Lebrun, J.L.; Morao Dias A. (1999): Residual stress analysis in orthogonal machining of standard and resulfurized AISI 316L steels. *Journal of Materials Processing Technology*, vol. 96 pp. 225-233.

Noyan, I.C.; Cohen, J.B. (1987): Residual stress Measurement by diffraction and interpretation, Springer-Verlag, New York.

Pawade, R.S.; Joshi, S. S.; Brahamnkar, P.K. (2008): Effect of machining parameters and cutting edge geometry on surface integrity of high speed turned Inconel 718. *Machine Tools & Manufacture*, vol. 48, pp. 15-28.

Sadat, A.B.; Reddy, M.Y. (1992): Surface integrity of Inconel 718 Nickel-base superalloy using controlled and natural contact length tools. Part 1: lubricated. *Experimental Mechanics*, vol. 32, no. 3, pp. 282-288.

Sadat, A.B.; Reddy, M.Y. (1993): Surface integrity of Inconel 718 Nickel-base superalloy using controlled and natural contact length tools. Part 2: unlubricated. *Experimental Mechanics*, vol. 33, no. 4, pp. 343-348.

Sharman, A.R.C; Hughes, J.I.; Ridgway, K. (2006): An analysis of the residual stresses generated in Inconel 718^{TM} when turning. *Journal of Materials Processing Technology*, vol. 173, pp. 359-367.

Society of Automotive Engineers (1971): Residual Stress Measurement by X-ray Diffraction, SAE J784, Society of Automotive Engineers, Inc., New York.

Valiorgue, F.; Rech, J.; Hamdi, H.; Gilles, P.; Bergheau, J.M. (2007): A new approach for modelling of residual stress induced by turning of 316L. *Journal of Materials Processing and Technology*, vol. 191, pp. 270-273.